

# Topological mechanics of gyroscopic metamaterials

Lisa M. Nash<sup>a</sup>, Dustin Kleckner<sup>a</sup>, Alismari Read<sup>a</sup>, Vincenzo Vitelli<sup>b</sup>, Ari M. Turner<sup>c,1</sup>, and William T. M. Irvine<sup>a,1</sup>

<sup>a</sup>James Franck Institute and Department of Physics, The University of Chicago, Chicago, IL 60637; <sup>b</sup>Instituut-Lorentz for Theoretical Physics, Universiteit Leiden, 2300 RA Leiden, The Netherlands; and <sup>c</sup>Department of Physics and Astronomy, Johns Hopkins University, Baltimore, MD 21218

Edited by David A. Weitz, Harvard University, Cambridge, MA, and approved October 13, 2015 (received for review April 17, 2015)

**Topological mechanical metamaterials are artificial structures whose unusual properties are protected very much like their electronic and optical counterparts. Here, we present an experimental and theoretical study of an active metamaterial—composed of coupled gyroscopes on a lattice—that breaks time-reversal symmetry. The vibrational spectrum displays a sonic gap populated by topologically protected edge modes that propagate in only one direction and are unaffected by disorder. We present a mathematical model that explains how the edge mode chirality can be switched via controlled distortions of the underlying lattice. This effect allows the direction of the edge current to be determined on demand. We demonstrate this functionality in experiment and envision applications of these edge modes to the design of one-way acoustic waveguides.**

topological mechanics | gyroscopic metamaterial | metamaterial

A vast range of mechanical structures, including bridges, covalent glasses, and conventional metamaterials, can be ultimately modeled as networks of masses connected by springs (1–6). Recent studies have revealed that despite its apparent simplicity, this minimal setup is sufficient to construct topologically protected mechanical states (7–11) that mimic the properties of their quantum analogs (12). This follows from the fact that, irrespective of its classic or quantum nature, a periodic material with a gapped spectrum of excitations can display topological behavior as a result of the nontrivial topology of its band structure (13–21).

All such mechanical systems, however, are invariant under time reversal because their dynamics are governed by Newton's second law, which, unlike the Schrödinger equation, is second order in time. If time-reversal symmetry is broken, as in recently suggested acoustic structures containing circulating fluids (16), theoretical work (13) has suggested that phononic chiral topological edge states that act as unidirectional waveguides resistant to scattering off impurities could be supported. In this paper, we show that by creating a coupled system of gyroscopes, a “gyroscopic metamaterial,” we can produce an effective material with intrinsic time-reversal symmetry breaking. As a result, our gyroscopic metamaterials support topological mechanical modes analogous to quantum Hall systems, which have robust chiral edge states (22–24). We demonstrate these effects by building a real system of gyroscopes coupled in a honeycomb lattice. Our experiments show long-lived, unidirectional transport along the edge, even in the presence of significant defects. Moreover, our theoretical analysis indicates that direction of edge propagation is controlled both by the gyroscope spin and the geometry of the underlying lattice. As a result, deforming the lattice of gyroscopes allows one to control the edge mode direction, offering unique opportunities for engineering novel materials.

Much of the counterintuitive behavior of rapidly spinning objects originates from their large angular momentum, which endows the axis of spin with a resistance to change. If we fix one end of a gyroscope and apply a force,  $\vec{F}$ , to the opposing free end of the spinning axis, we produce a torque of  $\vec{\tau} = \vec{\ell} \times \vec{F}$ , where  $\vec{\ell}$  is the axis of the gyroscope, pointing from the fixed to

the free end. In the fast spinning limit, the response of the gyroscope's axis is

$$\dot{\vec{\ell}} = \frac{\ell^2}{I\omega} (\vec{\ell} \times \vec{F}), \quad [1]$$

where  $\omega$  is the gyroscope angular frequency and  $I$  is its rotational inertia. The behavior of a gyroscope differs from that of a simple mass in two important ways: (i) It moves perpendicular to applied forces and (ii) its response is first order in time. The canonical example of this unusual behavior is precession: A spinning top does not simply fall over, but rather its free end orbits around the contact point (precesses) with a constant period,  $\Omega_g = mg\ell_{cm}/I\omega$ , where  $\ell_{cm}$  is the distance from the pivot point to center of gravity.

What happens if we replace the masses in a conventional mechanical metamaterial with gyroscopes? A first glimpse is provided by a normal mode analysis of honeycomb lattices composed of mass–spring and gyroscope–spring networks. The density of states of these two systems (Fig. 1A) shows qualitatively similar features: Each is characterized by two bands, a lower “acoustic” band (where neighboring sites move in phase) and an upper “optical” band (where neighboring sites move out of phase). The connections between these two bands, however, show key differences: In the mass–spring system the two bands touch at a Dirac point, whereas in the gyroscopic system a gap opens up between the bands. Crucially, this gap is not empty, but populated by nearly equally spaced modes and the number of these edge modes scales with the length of the edge. Examination of these gap modes reveals them to be confined to the edge and to be chiral: The phases always rotate in the same direction as one moves around the lattice (Fig. 1B). As we show below, these edge

## Significance

**We have built a new type of mechanical metamaterial: a “gyroscopic metamaterial” composed of rapidly spinning objects that are coupled to each other. At the edges of these materials, we find sound waves that are topologically protected (i.e. they cannot be scattered backward or into the bulk). These waves, which propagate in one direction only, are directly analogous to edge currents in quantum Hall systems. Through a mathematical model, we interpret the robustness of these edge waves in light of the subtle topological character of the bulk material. Crucially, these edge motions can be controlled by distorting the metamaterial lattice, opening new avenues for the control of sound in matter.**

Author contributions: L.M.N., D.K., V.V., A.M.T., and W.T.M.I. designed research; L.M.N., D.K., A.R., A.M.T., and W.T.M.I. performed research; L.M.N., D.K., A.R., A.M.T., and W.T.M.I. analyzed data; and L.M.N., D.K., V.V., A.M.T., and W.T.M.I. wrote the paper.

The authors declare no conflict of interest.

This article is a PNAS Direct Submission.

<sup>1</sup>To whom correspondence may be addressed. Email: aturne26@jhu.edu or wtmirvine@uchicago.edu.

This article contains supporting information online at [www.pnas.org/lookup/suppl/doi:10.1073/pnas.1507413112/-DCSupplemental](http://www.pnas.org/lookup/suppl/doi:10.1073/pnas.1507413112/-DCSupplemental).

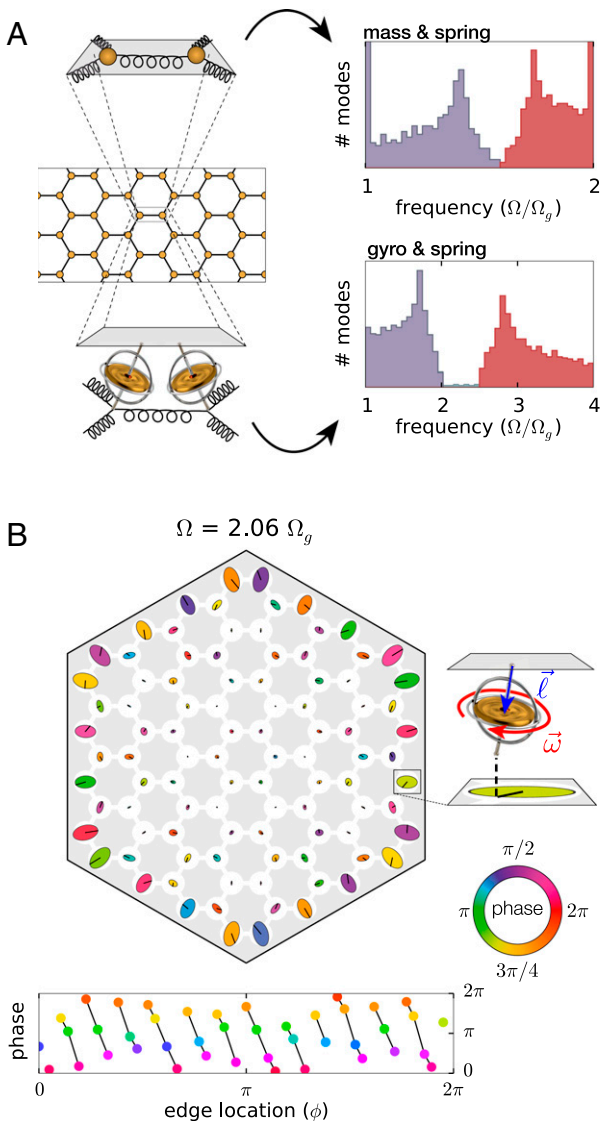


**Fig. 1.** Gyroscopic metamaterials and edge states. (A) A comparison between the density of states of a mass-spring (*Top*) and gyroscopic metamaterial (*Bottom*) on a honeycomb lattice. In both networks neighboring masses (gyroscopes) are coupled by springs and each mass (gyroscopic) feels a restoring force toward its equilibrium position. In the gyroscope network, the spring interaction frequency is  $\Omega_k = \Omega_g$ . The acoustic and optical bands of the network of masses connected by springs meet at a (Dirac) point. By contrast, in the network of gyroscopes connected by springs, there is a gap between acoustic and optical bands that is populated by chiral edge modes. (B) A normal mode (evaluated numerically) between the acoustic and optical bands in a lattice of 96 gyroscopes. The shape of each orbit in the normal mode is indicated with ellipses and the phase at a fixed time is indicated via color. The phase of the gyroscopes along the edge is indicated below, showing the phase velocity is unidirectional. This combined with the absence of a corresponding mode with opposite phase velocity is the key characteristic of chiral edge states.

modes are topologically robust and can therefore serve as unidirectional waveguides.

It is far from obvious that in a real system the phonon spectrum would be resistant to the presence of both disorder (lattice imperfections, gyroscopic nonuniformity, etc.) and mixed-order dynamics (e.g., nutation). However, an appealing feature of topological states is that they are often resistant to disorder, suggesting that they may be useful for acoustic applications and observable under a wide range of experimental conditions.

To explore the relevance of these effects, we have assembled a prototype system of 54 interacting gyroscopes on a honeycomb lattice (Fig. 2A and Fig. S2). Our gyroscopes consist of small dc motors spinning cylindrical masses at  $\sim 300$  Hz (with  $\sim 10\%$  variation in motor speed); each is suspended from a top plate by a weak spring (Fig. 2B), producing an individual precession frequency of  $\Omega_g \sim 1$  Hz. To couple these gyroscopes in a lattice, a small neodymium magnet is placed in each spinning mass with its moment aligned vertically, causing the gyroscopes to repel. For small displacements, this creates a linear effective spring-like force between gyroscopes that is comparable in strength to the gravitational pinning force.

The magnetically coupled system is conceptually equivalent to the system of gyroscopes connected by springs discussed earlier; the linearized magnetic coupling differs, however, in detail from the coupling given by springs because the equilibrium results from the cancellation of opposing forces instead of the absence of forces. As detailed in *Supporting Information*, this results in a mode spectrum that is shifted to lower frequencies (Fig. 2C), compared with a spring-coupled gyroscope system (Fig. 1A). However, the topological character of the band structure is not affected and acoustic and optical bands are still apparent with chiral edge modes in between.

To test the mechanical response of the gyroscopic metamaterial, we excite it with periodic bursts of air through a small nozzle and follow the resulting disturbance. We probe the normal modes by weakly exciting a single gyroscope at a fixed frequency for many ( $>100$ ) periods and recording the resulting motion of the network. All excitations were kept to small amplitudes ( $<10\%$  of the lattice spacing) to avoid the non-linearities associated with coupling the gyroscopes magnetically (Figs. S3–S5).

The effect of disorder inherent to our experiment (e.g., variation in motor speed and gyroscope pivot position) can be clearly seen in the comparison between the structure of bulk modes as shown in Fig. 2D and F for the idealized (*Left*) and experimental system (*Right*). There is little overall agreement between calculated and measured modes, though acoustic modes show approximate in-phase oscillation of adjacent gyroscopes and optical modes show approximate out-of-phase oscillation of adjacent gyroscopes. This is characteristic of the effects of disorder (25), which produces the same effect in numerically evaluated modes with comparable disorder (Fig. S6).

Despite these experimental imperfections, exciting a mode in the gap between the acoustic and optical bands produces clean excitations along the edge (Fig. 2E). The orientations and relative orbit sizes of these modes closely match the modes numerically computed for an idealized model. A comparison between calculated and measured edge mode frequencies is shown in Fig. S5. The robustness of these modes against disorder is characteristic of their topological character.

To demonstrate that our experimental metamaterial functions as a unidirectional waveguide, we excite a single edge gyroscope for five periods at a frequency in the gap. As shown in Fig. 3A and *Movie S1*, the resulting excitation propagates in only one direction around the edge of the lattice. The motion of this wave packet around the edge is persistent, circumnavigating the boundary several times. As expected, short excitations at a frequency not in the band gap do not produce a similar robust edge excitation (*Movie S2*). Crucially, this indicates that the chiral edge modes are topologically protected from coupling to the bulk modes, functioning as an efficient one-directional waveguide.

We further demonstrate the robustness of these edge modes by intentionally introducing disorder in the lattice, for example by removing three gyroscopes. As shown in *Movie S3* and Fig. 3B, even this significant disturbance does not destroy the chiral edge modes. An excitation on the edge is seen to move around

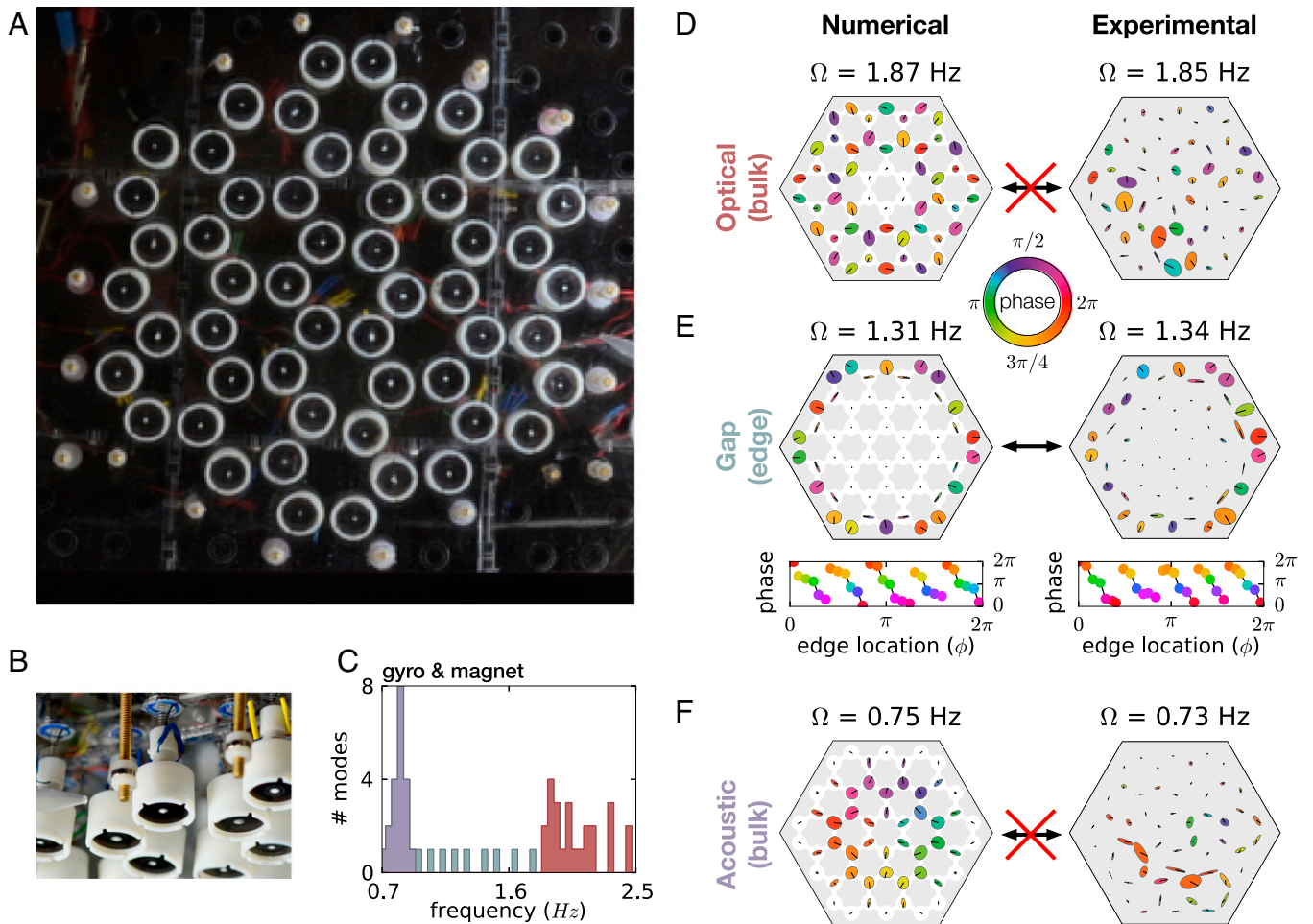


**Fig. 2.** Demonstration of robustness of edge modes in experiment. (A) A picture of the experimental system as viewed from below. (B) The edge of the experimental lattice from the side, showing the construction of the individual gyroscoopes as well as the fixed magnets around the edge that provide the lateral confinement. (C) The calculated histogram of normal mode frequencies for an array of 54 gyroscoopes arranged in a honeycomb lattice (no disorder) is shown. The frequencies range from 0.7 to 2.5 Hz. (D–F) A comparison of calculated normal modes in an ideal magnetic-gyroscope network (Left) as measured in an experimental system (Right). For each system a mode is shown in (D) the optical band, (E) the band gap, and (F) the acoustic band. Disorder has a strong effect on bulk mode profiles. However, the gap mode profiles correspond much more closely to the ideal modes in shape, orientation, and phase of the gyroscope orbits.

this disturbance—in the same direction as before—and emerge undisturbed on the other side. Remarkably, the excitation traverses the defect region without scattering backward or into the bulk. As before, the resilience of the edge modes suggests these edge states are topological in character.

To analyze the origin of these effects, we return to an ideal coupled gyroscope model. For simplicity, we represent the displacement of the tip of the gyroscope from equilibrium as  $\psi \rightarrow \delta_x + i\delta_y$ . In this form, the linearized version of Eq. 1 is  $i(d\psi/dt) = (\ell^2/I\omega)F$ , where  $F \rightarrow F_x + iF_y$  is the complex representation of the interaction force and the complex phase,  $i$ , arises from the cross-product. Accordingly, the linearized equation of motion for each site in the gyroscopic metamaterial is

$$i \frac{d\psi_p}{dt} = \Omega_g \psi_p + \frac{1}{2} \sum_{q \in n.n.(p)} \left[ \left( \Omega_{pp}^+ \psi_p + \Omega_{pq}^+ \psi_q \right) + e^{2i\theta_{pq}} \left( \Omega_{pp}^- \psi_p^* + \Omega_{pq}^- \psi_q^* \right) \right], \quad [2]$$

where  $p$  is the site label,  $q$  the neighboring sites,  $\theta_{pq}$  is the spring bond angle, and  $\Omega_{pq}^\pm = -\frac{\ell^2}{I\omega} (\partial F_{p\parallel} / \partial x_{j\parallel} \pm \partial F_{p\perp} / \partial x_{j\perp})$  are determined from gradients of the force on  $p$ ,  $F_p$ , parallel and perpendicular

to the line connecting the equilibrium positions of the gyroscoopes. In the case of the interactions being provided by springs,  $\Omega_{pq}^\pm = k\ell^2/I\omega = \Omega_k$ , where  $k$  is the spring constant.

Symmetries often play a fundamental role in characterizing a system's topological behavior; in the case of the gyroscopic materials, broken time-reversal symmetry is a natural starting point. We note that the linearized equation of motion bears remarkable similarity to the Schrödinger equation for the wavefunction of an electron in a tight-binding model. Thus, by analogy, we may analyze the breaking of temporal symmetry using the “time-reversal” operation in quantum mechanics:  $t \rightarrow -t$ ,  $\psi \rightarrow \psi^*$ . For gyroscoopes, conjugating  $\psi$  mirrors their displacement in the  $y$  axis; applying the complete time-reversal operation to a single gyroscope leaves the equation of motion unchanged. Similarly, for a network of gyroscoopes Eq. 2 is invariant under this operation only if the coefficient  $e^{2i\theta_{pq}}$  is real (up to a global rotation), and breaks the symmetry otherwise. Thus, crucially, we see that the breaking of time-reversal symmetry depends on distribution of bond angles in the lattice, and not simply the response of individual gyroscoopes.

The geometric origin of the time-reversal symmetry breaking can also be seen in the case of gyroscoopes connected by springs,



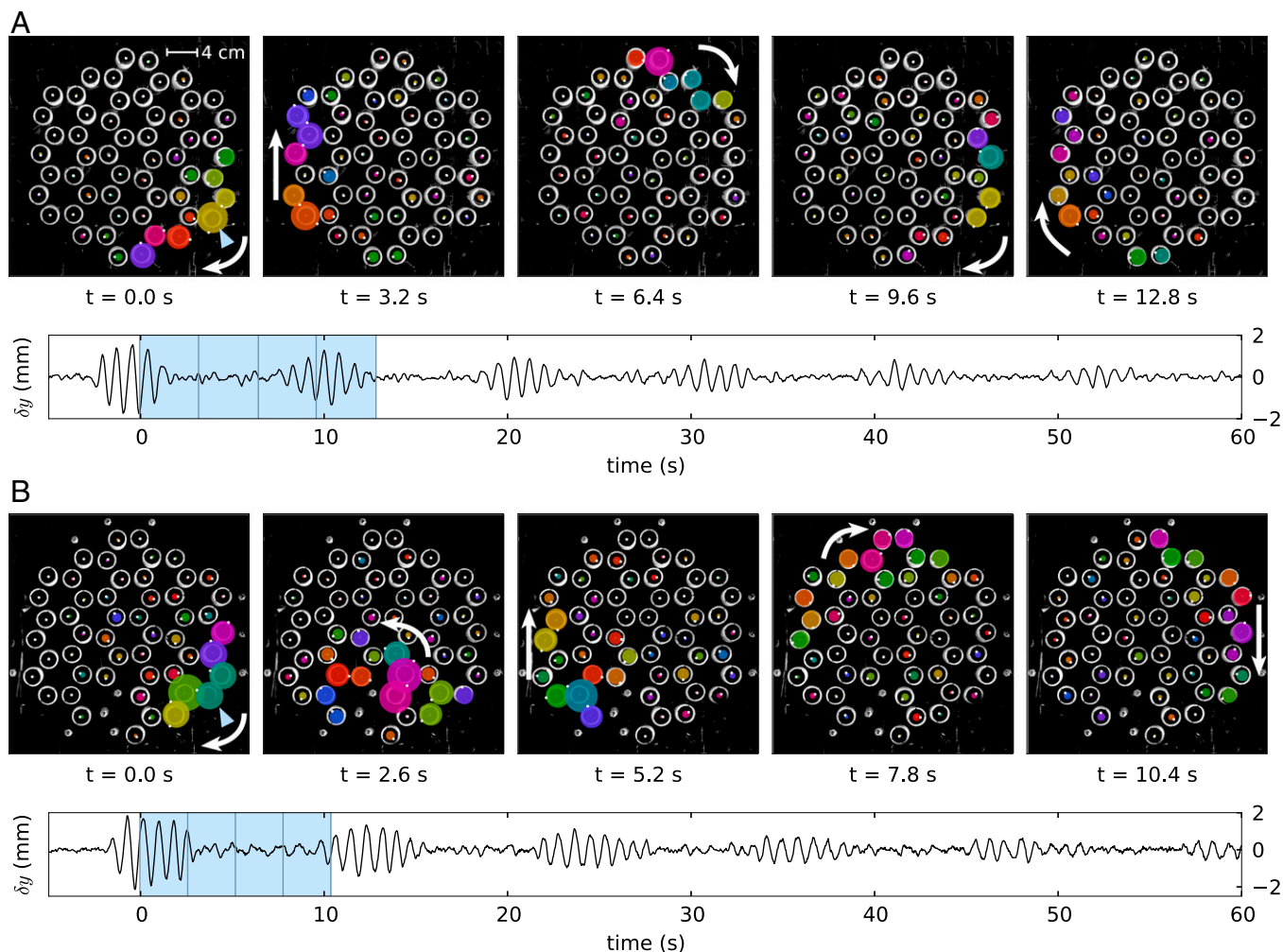


**Fig. 3.** Unidirectional waveguide modes in experiment. (A) A single edge gyroscope is excited for five periods; subsequent images show the excitation propagation clockwise around the edge. The bottom graph indicates the displacement of one gyroscope (indicated with a triangle) in the y direction; the excitation is seen to persist for many cycles around the edge. (B) The same experiment as in A, but with three gyroscopes removed from the bottom edge and replaced with fixed magnets (to keep the system in equilibrium). Owing to the topological nature of the edge modes, the excitation propagates around the disturbance.

by considering the energy of two connected gyroscopes. In the linearized limit, the stretching/compression of the spring is given by  $\Delta \propto (r_{x1} - r_{x2})\cos\theta_{12} + (r_{y1} - r_{y2})\sin\theta_{12}$ . If we mirror each gyroscope in the y axis ( $\psi \rightarrow \psi^*$  or  $r_y \rightarrow -r_y$ ), in general the spring length will be unchanged only if  $\sin\theta_{12} = 0$  (i.e., if the mirror axis aligns with the equilibrium bond angle). However, if  $\cos\theta_{12} = 0$ , or the mirroring axis is perpendicular to the bond, then the spring energy,  $E_k \propto \Delta^2$ , is conserved by converting stretching to compression (Fig. 4A). When considering an entire lattice, we see that for arbitrary displacements the bond energy will be conserved under time reversal if (and only if) we are able to choose a global mirror axis to which all bonds are either perpendicular or parallel. As a result, time-reversal invariance is only guaranteed for lattices composed of square or rectangular building blocks.

It is instructive to note that, in the limit that gyroscopes are coupled by weak springs,  $\Omega_k \ll \Omega_g$  our gyroscopic metamaterial has a well-known quantum-mechanical analog: the Haldane model of an electronic system in a honeycomb lattice (see *Supporting Information* and *Figs. S7* and *S8* for details) (26). In the Haldane model, time-reversal symmetry is broken by a staggered magnetic field. This field can be varied, resulting in a change in the topological character of the modes

as quantified by the Chern number (12, 27, 28). Accordingly, depending on the strength of the field and asymmetry between the two sites in the unit cell, the Chern number of the bottom band is  $C_- = 0, \pm 1$ , and  $C_+ = -C_-$  in the top band. A Chern number of zero indicates a trivial topology (a normal insulator), whereas a nonzero Chern number indicates a non-trivial topology. Whenever  $C_{\pm} \neq 0$ , topological edge modes appear in the gap between the two bands; the chirality and direction of propagation of these modes depends on the sign of the Chern number for lower band.

In gyroscopic metamaterials, the analog to changing the magnetic field is to geometrically distort the lattice. In either case, the relevant operation produces a phase shift in the hopping between neighboring sites; in the gyroscope system this phase shift is determined by the bond angles,  $\theta_{pq}$ . In the case of an undistorted honeycomb lattice, the modes have a Chern number of  $C_{\pm} = \pm 1$ , in agreement with the Haldane model.

In a honeycomb lattice, it is possible to distort the constituent hexagons without changing the bond length (Fig. 4 B–D), allowing us to change the gyroscopic phase between neighboring sites without changing the network connectivity. As predicted by the time-reversal analysis above, the band-gap and chiral edge modes disappear when the bonds fall on a rectangular grid (in

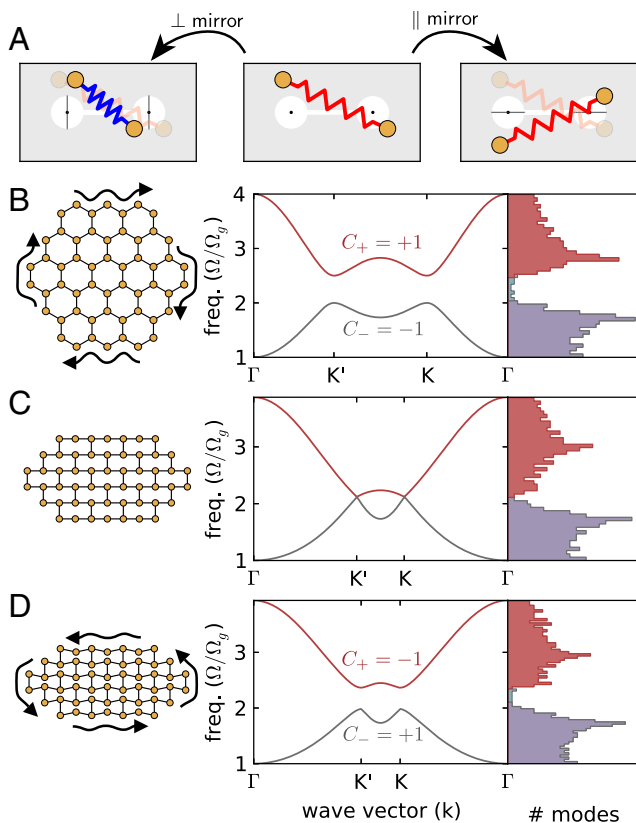


**Fig. 4.** Controlling time-reversal invariance in a gyroscopic metamaterial. (A) The effect of mirroring a configuration of two gyroscopes around axes that are perpendicular or parallel to the equilibrium bond angle. Mirroring about axes that are perpendicular to the bond angle (Left) converts stretching to compression but conserves the energy stored in the bond. Mirroring about the axes that are parallel to the bond (Right) conserves the total bond length. Mirroring about other axes, in general, does not conserve energy. (B–D) For each lattice geometry (Left), the band structure for an infinite system is shown (Middle) along with the density of states for a finite lattice of 726 gyroscopes (Right). (B) An undisturbed, hexagonal honeycomb lattice. (C) A honeycomb lattice as it is distorted into a rectangular configuration while preserving the connectivity. (D) A honeycomb lattice distorted past the square configuration. The rectangular configuration has no band gap, and consequently no edge modes; as the lattice is further distorted the band gap reopens but the edge modes have opposite chirality.

which case  $e^{2i\theta_{pq}} = \pm 1$ ). Furthermore, the dispersion relationship of an infinite gyroscopic lattice in this configuration has Dirac

points at the corners of the Brillouin zone (Fig. 4C); this is topologically equivalent to the dispersion relationship of a honeycomb network of springs and masses. Continuing to distort the lattice past this point restores the band gap, but the edge modes now have opposite chirality, as reflected in an inversion of the bands and hence of the Chern number;  $C_{\pm} = \mp 1$ . As a result, excitations along the edge now move in the other direction, opposite to the precession of individual gyroscopes. These effects can all be seen in [Movies S4](#) and [S5](#). [Movie S4](#) shows the simulated dynamics of an edge mode in a spring coupled gyroscopic metamaterial as it is being distorted. Remarkably, this indicates the direction of the edge waveguide can be controlled purely through geometric distortions of the lattice, analogous to an effect recently observed in 1D acoustic phononic crystals (29).

We have presented an experimental proof of concept and theoretical analysis of a topologically protected unidirectional waveguide in a real mechanical metamaterial. The origin of our topological edge modes is due to time-reversal symmetry breaking; our analysis indicates this arises from the combination of the chiral nature of the gyroscopes and the geometry of the underlying lattice. Because the direction of the edge modes can be changed discontinuously with geometric distortions, in principle small displacements should be capable of inverting the edge mode direction. This mechanism may have practical applications for creating direction-tunable materials, but it also suggests interesting nonlinear effects should occur in the regime near the mechanically induced topological phase transition.

The prototypical gyroscopic solids we have developed here are examples of active metamaterials: Their design relies on the presence of internal motors that keep each gyroscope in a fast spinning state. An open challenge is to construct scalable gyroscopic metamaterials using nanofabrication techniques (e.g., microelectromechanical systems) or active molecules that convert chemical energy into rotation very much like the motors powering each gyroscope (30, 31). Such an implementation would pave the way toward realizing materials that support, at a microscopic scale, robust topological acoustic modes.

**Note Added in Proof.** In the concluding stages of the present work, we became aware of a parallel independent effort in which a class of topological gyroscopic metamaterials was theoretically analyzed (32).

**ACKNOWLEDGMENTS.** We acknowledge the Materials Research and Engineering Centers (MRSEC) Shared Facilities at The University of Chicago for the use of their instruments. This work was supported by the National Science Foundation MRSEC Program at The University of Chicago (Grant DMR-1420709). W.T.M.I. acknowledges support from the A. P. Sloan Foundation through a Sloan Fellowship and the Packard Foundation through a Packard Fellowship.

- Maxwell JC (1864) On the calculation of the equilibrium and stiffness of frames. The London, Edinburgh, and Dublin Philosophical Magazine and Journal of Science 27(182):294–299.
- Wei ZY, Guo ZV, Dudte L, Liang HY, Mahadevan L (2013) Geometric mechanics of periodic pleated origami. *Phys Rev Lett* 110(21):215501.
- Thorpe MF (1983) Continuous deformations in random networks. *J Non-Cryst Solids* 57(3):355–370.
- Wyart M, Nagel SR, Witten TA (2005) Geometric origin of excess low-frequency vibrational modes in weakly connected amorphous solids. *Europhys Lett* 72(3):486–492.
- Lubensky TC, Kane CL, Mao X, Souslov A, Sun K (2015) Phonons and elasticity in critically coordinated lattices. *Rep Prog Phys* 78(7):073901.
- Kang SH, et al. (2014) Complex ordered patterns in mechanical instability induced geometrically frustrated triangular cellular structures. *Phys Rev Lett* 112(9):098701.
- Kane CL, Lubensky TC (2013) Topological boundary modes in isostatic lattices. *Nat Phys* 10(1):39–45.
- Paulose J, Chen BG-g, Vitelli V (2015) Topological modes bound to dislocations in mechanical metamaterials. *Nat Phys* 11(2):153–156.
- Chen BG, Upadhyaya N, Vitelli V (2014) Nonlinear conduction via solitons in a topological mechanical insulator. *Proc Natl Acad Sci USA* 111(36):13004–13009.
- Paulose J, Meeussen AS, Vitelli V (2015) Selective buckling via states of self-stress in topological metamaterials. *Proc Natl Acad Sci USA* 112(25):7639–7644.
- Vitelli V, Upadhyaya N, Chen BG-g (2014) Topological mechanisms as classical spinor fields. arXiv:1407.2890 [cond-mat.soft].
- Hasan MZ, Kane CL (2010) Colloquium: Topological insulators. *Rev Mod Phys* 82(4):3045–3067.
- Prodan E, Prodan C (2009) Topological phonon modes and their role in dynamic instability of microtubules. *Phys Rev Lett* 103(24):248101.
- Wang Z, Chong Y, Joannopoulos JD, Soljacic M (2009) Observation of unidirectional backscattering-immune topological electromagnetic states. *Nature* 461(7265):772–775.
- Berg N, Joel K, Koolyk M, Prodan E (2011) Topological phonon modes in filamentary structures. *Phys Rev E Stat Nonlin Soft Matter Phys* 83(2 Pt 1):021913.
- Yang Z, et al. (2015) Topological acoustics. *Phys Rev Lett* 114(11):114301.
- Hafezi M, Mittal S, Fan J, Migdall A, Taylor JM (2013) Imaging topological edge states in silicon photonics. *Nat Photonics* 7(12):1001–1005.
- Rechtsman MC, et al. (2013) Photonic Floquet topological insulators. *Nature* 496(7444):196–200.
- Süsstrunk R, Huber SD (2015) PHYSICS. Observation of phononic helical edge states in a mechanical topological insulator. *Science* 349(6243):47–50.
- Peano V, Brendel C, Schmidt M, Marquardt F (2015) Topological phases of sound and light. *Phys Rev X* 5(3):031011.
- Ningyuan J, Owens C, Sommer A, Schuster D, Simon J (2015) Time- and site-resolved dynamics in a topological circuit. *Phys Rev X* 5(2):021031.
- Haldane FDM, Raghu S (2008) Possible realization of directional optical waveguides in photonic crystals with broken time-reversal symmetry. *Phys Rev Lett* 100(1):013904.

23. Raghu S, Haldane F (2008) Analogs of quantum-hall-effect edge states in photonic crystals. *Phys Rev A* 78(3):033834.
24. Wang Z, Chong YD, Joannopoulos JD, Soljacić M (2008) Reflection-free one-way edge modes in a gyromagnetic photonic crystal. *Phys Rev Lett* 100(1):013905.
25. Maradudin AA (1965) Some effects of point defects on the vibrations of crystal lattices. *Reports on Progress in Physics* 28(1):331–380.
26. Haldane FD (1988) Model for a quantum Hall effect without Landau levels: Condensed-matter realization of the “parity anomaly”. *Phys Rev Lett* 61(18):2015–2018.
27. Avron JE, Seiler R, Simon B (1983) Homotopy and quantization in condensed matter physics. *Phys Rev Lett* 51(1):51–53.
28. Thouless DJ, Kohmoto M, Nightingale MP, den Nijs M (1982) Quantized hall conductance in a two-dimensional periodic potential. *Phys Rev Lett* 49(6):405–408.
29. Xiao M, et al. (2015) Geometric phase and band inversion in periodic acoustic systems. *Nat Phys* 11(3):240–244.
30. Prost J, Jülicher F, Joanny JF (2015) Active gel physics. *Nat Phys* 11(2):111–117.
31. Palacci J, Sacanna S, Steinberg AP, Pine DJ, Chaikin PM (2013) Living crystals of light-activated colloidal surfers. *Science* 339(6122):936–940.
32. Wang P, Lu L, Bertoldi K (2015) Topological phononic crystals with one-way elastic edge waves. *Phys Rev Lett* 115:104302.
33. Molerón M, Leonard A, Daraio C (2014) Solitary waves in a chain of repelling magnets. *J Appl Phys* 115(18):184901.